Title
Multiple signaling systems target a core set of transition metal homeostasis genes using similar binding motifs

Authors
Garber, Megan E
Rajeev, Lara
Kazakov, Alexey E
et al.

Multiple signaling systems target a core set of transition metal homeostasis genes using similar binding motifs

Megan E. Garber,[1,2][†] Lara Rajeev,[1][†]
Alexey E. Kazakov,[3] Jessica Trinh,[1] Duy Masuno,[1]
Mitchell G. Thompson,[1,3,4] Nurgul Kaplan,[1]
Joyce Luk,[1] Pavel S. Novichkov[3,5] and
Aindrila Mukhopadhyay 🆔[1,3][*]

[1]*Biological Systems and Engineering Division, Lawrence Berkeley National Laboratory, Berkeley, CA 94720, USA.*
[2]*Department of Comparative Biochemistry, University of California, Berkeley, CA 94720, USA.*
[3]*Environmental Genomics and Systems Biology Division, Lawrence Berkeley National Laboratory, Berkeley, CA 94720, USA.*
[4]*Department of Plant and Microbial Biology, University of California, Berkeley, CA 94720, USA.*
[5]*Department of Energy, Knowledge Base, Lawrence Berkeley National Laboratory, Berkeley, CA 94720, USA.*

Summary

Bacterial response to metals can require complex regulation. We report an overlapping regulation for copper and zinc resistance genes in the denitrifying bacterium, *Pseudomonas stutzeri* RCH2, by three two-component regulatory proteins CopR1, CopR2 and CzcR. We conducted genome-wide evaluations to identify gene targets of two paralogous regulators, CopR1 and CopR2, annotated for copper signaling, and compared the results with the gene targets for CzcR, implicated in zinc signaling. We discovered that the CopRs and CzcR have largely common targets, and crossregulate a core set of *P. stutzeri* copper and zinc responsive genes. We established that this crossregulation is enabled by a conserved binding motif in the upstream regulatory regions of the target genes. The crossregulation is physiologically relevant as these regulators synergistically and antagonistically target multicopper oxidases, metal efflux and sequestration systems. CopR1 and CopR2 upregulate two *cop* operons encoding copper

tolerance genes, while all three regulators downregulate a putative copper chaperone, Psest_1595. CzcR also upregulated the *oprD* gene and the CzcIABC Zn^{2+} efflux system, while CopR1 and CopR2 downregulated these genes. Our study suggests that crossregulation of copper and zinc homeostasis can be advantageous, and in *P. stutzeri* this is enabled by shared binding motifs for multiple response regulators.

Introduction

Pseudomonas stutzeri RCH2 is a denitrifying bacterium isolated from the United States Department of Energy Superfund site at Hanford (Chakraborty *et al.*, 2017). High levels of chromate and other heavy metals are the primary selectors of microbial function and microbial community architecture (Lin *et al.*, 2012; Somenahally *et al.*, 2013) and influence the overall biological metal homeostasis at such sites. *P. stutzeri* RCH2 (hereafter referred to as RCH2) is emerging as a model organism to study denitrification and metal reduction under various redox regimes (Lalucat *et al.*, 2006; Thorgersen *et al.*, 2015). RCH2 is also of interest for its novel metal cation resistance genes (Vaccaro *et al.*, 2016). Although the annotated genome of RCH2 and other isolates from these environments often encode multiple signaling systems for response to a range of metals, these signal transduction cascades and their relation to each other is poorly delineated. Transition metals like copper are known to be some of the most pervasive contaminants with known antimicrobial function, and are pertinent not only to contamination sites but broadly to most microbial environments (Ladomersky and Petris, 2015; Chandrangsu *et al.*, 2017). The copper responsive genes in RCH2 genome are most alike the copper resistance systems of pathogens such as *P. aeruginosa* (Cha and Cooksey, 1991).

RCH2 contains a remarkable number of redundant metal homeostasis genes, and notably contains two paralogous signaling systems for copper response (Vaccaro *et al.*, 2016). A recent study using RCH2 RB-Tnseq libraries has shown that in this bacterium numerous operons and regulators are involved in response to elevated concentrations of copper and zinc cations (Vaccaro *et al.*, 2016). At the same time, several known copper resistance genes (e.g.,

copA1, copB1, copA2, copB2) did not demonstrate a copper-specific phenotype in that study. Transition metals are known to have interrelated and complex impact on microbial physiology often triggering overlapping response (Singh *et al.*, 2014). Coordinated interactions may be required for the optimal final response and has been reported for the copper- and zinc-responsive regulators in *P. aeruginosa* (Caille *et al.*, 2007) and copper-responsive regulators in *Salmonella* sp (Pezza *et al.*, 2016). However, neither the copper nor the zinc responsive signaling is understood in a *P. stutzeri* strain, which serves as the physiological model for denitrification and metal tolerance. In this study, we examined two paralogous response regulators (RR), CopR1 and CopR2 that are part of two putative two-component signaling systems (TCS) in RCH2. We have also examined CzcR, a two-component RR implicated in zinc response (Vaccaro *et al.*, 2016).

For these three RRs, specifically CopR1, CopR2 and CzcR, we used purified His-tagged proteins to conduct a DAP-seq (DNA Affinity-Purified-seq) evaluation. Our previous DAP-chip examination of all transcriptionally acting RRs of a model sulfate reducer (Rajeev *et al.*, 2011; Rajeev *et al.*, 2014) had successfully revealed interconnectivities in regulatory modules that typically elude studies focused on a single TCS. A DAP-seq approach allowed us to examine all gene targets of the three RRs in RCH2. Our main finding is that most gene targets of the copper and zinc responsive TCSs are shared, and

are regulated by all three regulators due to similar binding motifs upstream of these targets. The specific outcome of crossregulation is different from what has been reported for other bacteria (Caille *et al.*, 2007; Pezza *et al.*, 2016), but its occurrence suggests it to be a common phenomenon present more broadly in bacteria. We present these results as well as validation of the physiological and context dependent relevance of these findings.

Results and Discussion

RCH2 encodes two sets of genes annotated for copper tolerance functions with two paralogous (84% identical amino acid sequences) copper responsive RRs, CopR1 (Psest_0581) and CopR2 (Psest_1598) (Vaccaro *et al.*, 2016; Chakraborty *et al.*, 2017). Copper is one of the most prevalent trace element contaminants and presents a well-known antimicrobial challenge, but is also essential for denitrification and aerobic growth (Ladomersky and Petris, 2015). The genomic context shows several copper related genes co-localized with the two RRs. Chromosomal proximity implicates CopR1 in the regulation of Psest_0582, Psest_0583–0586 encoding CopA1, CopB1 [putative multicopper oxidase and outer membrane proteins that are homologs of the *P. syringae* copper resistance proteins (Cha and Cooksey, 1991; Hoegger *et al.*, 2006; Rowland and Niederweis, 2013)] and Psest_0585 (CopM1), a
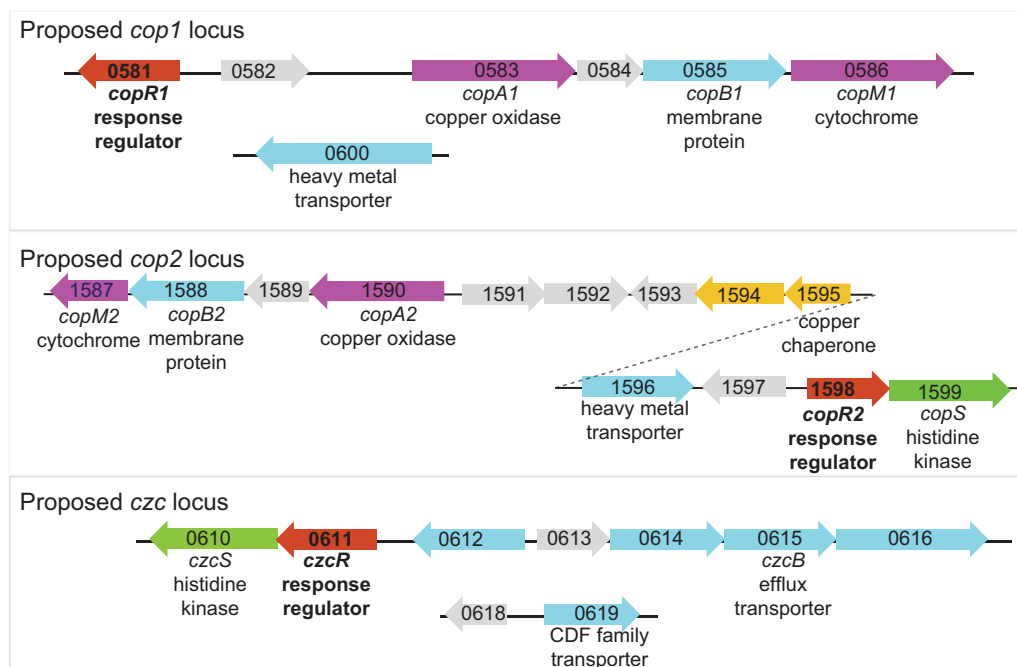
Fig. 1. Genomic context of *copR1, copR2, czcR*. Depiction of the orientation of *copR1, copR2* and *czcR* and their proposed regulatory gene targets as described in Vaccaro *et al.* (2016). The genes are functionally annotated as: blue for transport, yellow for sequestration, magenta for oxidases, gray for hypothetical or unknown function, red for RRs and green for HKs.

Table 1. DAP-seq evaluation of CopR1, CopR2 and CzcR.

| CopR1	CopR2	CzcR	Overlapping peak	Gene name	Function
+	+	+	Psest_0581	*copR1*	Heavy metal response regulator
+	+	+	Psest_0582		Hypothetical protein
−	+	+	Psest_0583	*copA1*	Copper oxidase
−	+	+	Psest_0584		Hypothetical protein
−	+	+	Psest_0585	*copB1*	Membrane protein (hypothetical transporter)
−	+	+	Psest_0586	*copM1*	Cytochrome
−	−	+	Psest_0587		Domain of conserved function (DUF326)
+	+	+	Psest_0589		Uncharacterized protein
+	+	+	Psest_0600		Heavy metal transporter
−	−	+	Psest_0610	*czcS*	Heavy metal sensor kinase
−	−	+	Psest_0611	*czcR*	Heavy metal response regulator
+	+	+	Psest_0612	*oprD*	Outer membrane porin, OprD
+	+	+	Psest_0613	*czcI*	Hypothetical protein
+	+	+	Psest_0614	*czcA*	Outer membrane protein
+	+	+	Psest_0615	*czcB*	RND family efflux transporter
+	+	+	Psest_0616	*czcC*	Heavy metal efflux pump (cobalt-zinc-cadmium)
+	+	+	Psest_0618		Hypothetical protein
+	+	+	Psest_0619		CDF family transporter
+	+	+	Psest_1587	*copM2*	Cytochrome
+	+	+	Psest_1588	*copB2*	Membrane protein (hypothetical transpoter)
+	+	+	Psest_1589		Hypothetical protein
+	+	+	Psest_1590	*copA2*	Copper oxidase
+	+	+	Psest_1591		Hypothetical protein
+	+	+	Psest_1592		Hypothetical protein
+	+	+	Psest_1593		Hypothetical protein
+	+	+	Psest_1594		Predicted metal-binding protein
+	+	+	Psest_1595		Copper chaperone
+	+	+	Psest_1596		ATPase P-type (transporting)
+	+	+	Psest_1597		Protein of unknown function (DUF2933)
+	+	+	Psest_1598	*copR2*	Heavy metal response regulator
+	+	+	Psest_1599	*copS*	Heavy metal sensor kinase

Major DAP-seq hits for CopR1, CopR2 and CzcR. If CopR1, CopR2 or CzcR targeted a gene (Psest_xxxx) under any DAP-seq experimental condition, it is denoted with a plus (+). These loci share at least a single copy of the same motif upstream of the coding sequence of the first gene in an operon. The complete list of DAP-seq hits under all experimental conditions targets can be found in Supporting Information data tables.

putative cytochrome (Fig. 1). Similarly, CopR2 is proximal to Psest_1597, Psest_1596, Psest_1595-91, Psest_1590-1587 encoding, among other proteins, a second multicopper oxidase CopA2 (Psest_1590), CopB2 (Psest_1588) and CopM2 (Psest_1587) and a putative copper chaperone (Psest_1595). However, recent fitness data from a RB-TnSeq library of RCH2 reveals a much larger number of genes to be involved in copper homeostasis (Vaccaro *et al.*, 2016).

To comprehensively examine the genes being targeted by these two paralogous TCSs, we purified the CopR1 and CopR2 RRs and subjected them to a DAP-seq evaluation (Experimental procedures, Supporting Information Fig. S1). DAP-seq uses purified RRs to enrich the DNA sequences they have affinity for in an *in vitro* setting (Rajeev *et al.*, 2011; Rajeev *et al.*, 2014; O'Malley *et al.*, 2016). The statistical analysis and cut-offs used to set the threshold for candidates considered for further evaluation are described in the experimental procedures section. Confidently assigned enriched DNA allowed the identification of the potential gene targets that are regulated by these RRs.

Our DAP-seq results showed a large overlap in the gene targets for CopR1 and CopR2 (Table 1, Fig. 2A, Supporting Information). One of the *copABM* operons (Psest_1590-1587) and homologs of other known copper resistance genes [Psest_0600, Psest_1597 (Caille *et al.*, 2007; Long *et al.*, 2010; Su *et al.*, 2011)], are targeted by both CopR1 and CopR2. Genes encoding the two CopR RRs (Psest_0581 and Psest_1598) were also targeted by both CopR1 and CopR2, as were a few other genes encoding hypothetical proteins and proteins of unknown functions. CopR targets also included Psest_1595-1593 operon encoding putative copper chaperone and putative metal-binding protein, Psest_0600 and Psest_1596 both putative heavy-metal transporters. As listed in Table 1, the only set of high confidence enriched genes for CopR2 that were not CopR1 targets were in the Psest_0583-6 operon that includes the *copA1*, Psest_0584 (encoding a protein of unknown function), *copB1* and *copM1* genes.

Most strikingly, both CopR1 and CopR2 bound and enriched upstream regions of genes annotated for zinc response and transport. These include the outer
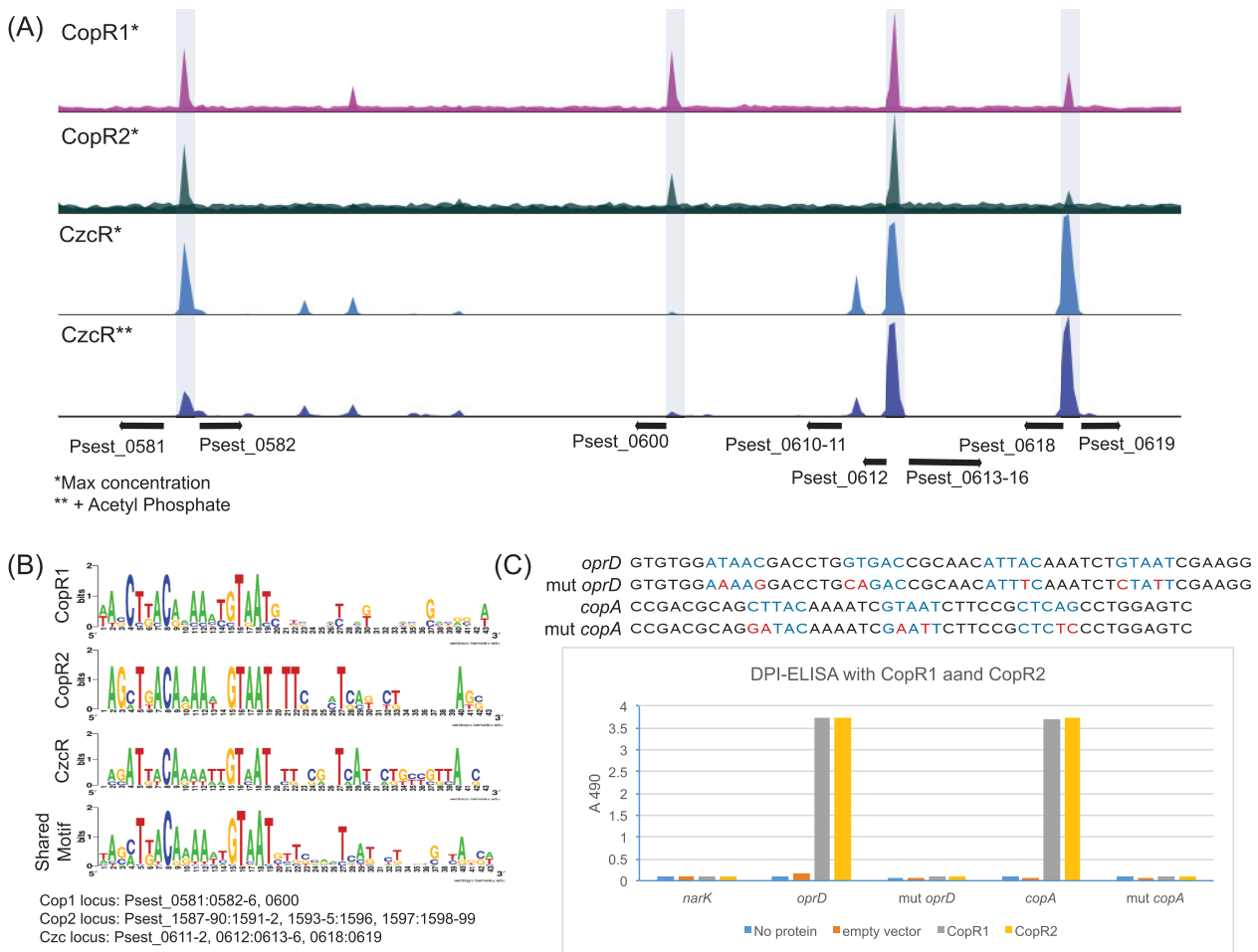
Fig. 2. Upstream region of DAP-seq targets contain canonical binding motifs.

A. Overlapping peaks for enriched gene loci for CopR1 (magenta), CopR2 (green) and CzcR (blue) and their corresponding gene targets found with DAP-seq. See Supporting Information data for DAP-seq targets under all conditions tested.

B. Consensus sequence of binding motifs as generated by Weblogo (Crooks *et al.*, 2004) for proposed distinct loci (Vaccaro *et al.*, 2016) for CopR1, CopR2 and CzcR, and a motif logo of the shared binding motif for all three regulators.

C. DPI-ELISA showed that CopR1 and CopR2 bound to the motif upstream of *copA* (Psest_1590) and also to the predicted CzcR binding motif upstream of *oprD* (Psest_0612). Substitutions (in red font) in the conserved base pairs (blue font) in the CopR and CzcR binding motifs eliminated the binding (mut *oprD* and mut *copA*). As a control, binding was tested against an unrelated NarL motif upstream of *narK*. The empty vector extract did not bind any of the sites tested.

membrane porin gene *oprD* (Psest_0612), the *czcIABC* operon for RND-type zinc-cadmium-cobalt efflux transporter (Psest_0613-16) and Psest_0618 (encoding a hypothetical protein that has been identified as required for fitness during zinc stress (Vaccaro *et al.*, 2016)) (Table 1, Supporting Information). These genes are also predicted to be regulated by the zinc responsive TCS CzcRS. The overall percent identity of CzcR to CopR1 and CopR2 is 55% and 59% respectively. To examine the role of CzcR in this regulatory map, we purified CzcR (Psest_0611) and conducted a DAP-seq analysis on this RR. In contrast to the CopR1 and CopR2 DAP-seq, which enriched 8–15 target loci corresponding to 30–50 genes, CzcR enriched a very large number of targets corresponding to hundreds of genes, including

many genes that were also enriched in the CopR1 and CopR2 DAP-seqs. For each RR, DAP-seq was conducted with and without the addition of acetyl phosphate; however, the high-confidence target genes identified were the same regardless of the addition of this reagent. A complete list of DAP-seq targets for all 3 RRs under all testing conditions is provided in the Supporting Information section. Analysis of the upstream regions of genes in the DAP-seq data revealed very similar motifs for genes targeted by the three RRs (Fig. 2B). We confirmed the specificity of the binding motif with DPI-ELISA assays with native and altered (mutant) DNA sequences with CopR1 and CopR2 (Fig. 2C). Base pair modifications of the conserved positions in these motifs were sufficient to disrupt the DNA-
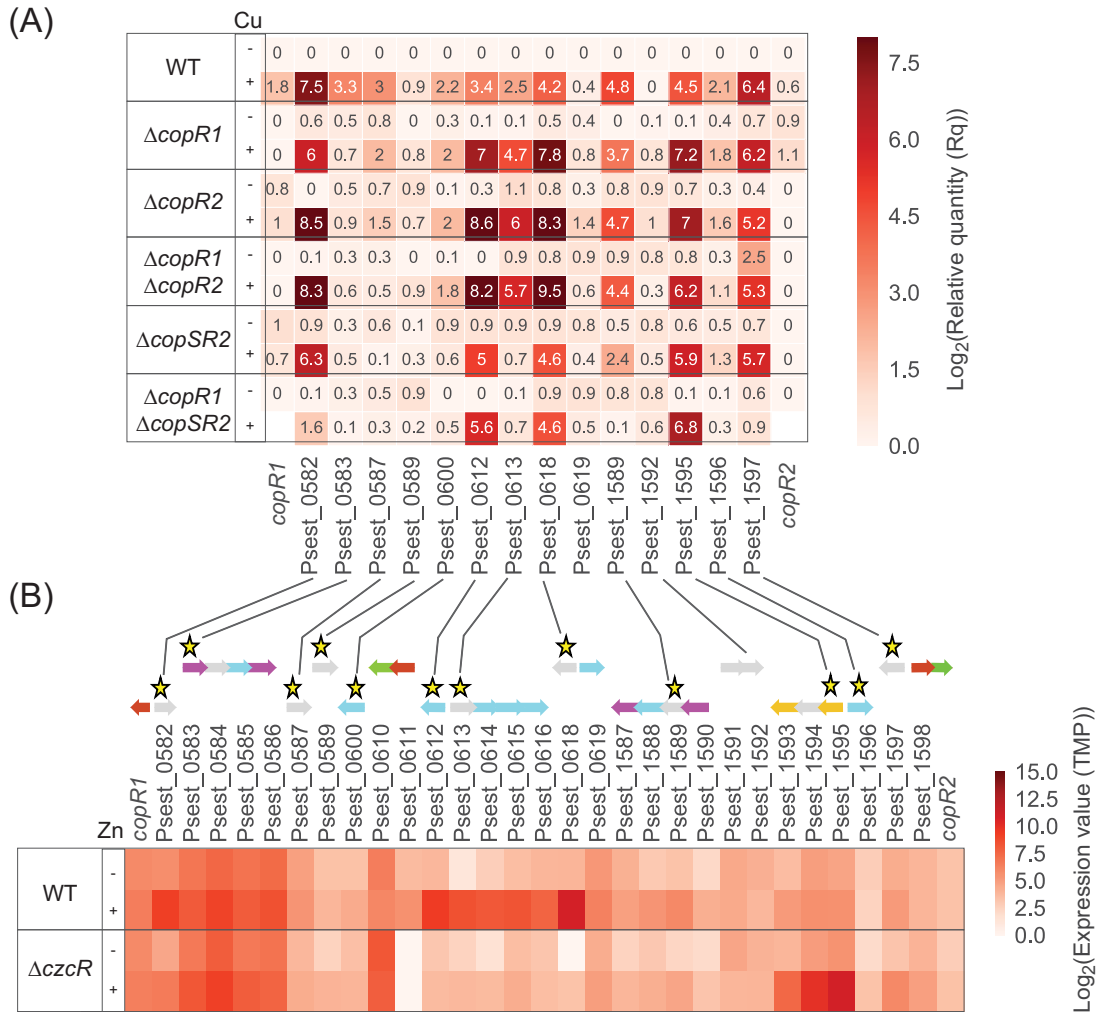
Fig. 3. Response of gene targets *in vivo*. Differential expression patterns exhibited by *copR* and *czcR* knockouts.
A. Heatmap of the log$_2$ relative expression (Rq) as determined by qRT-PCR for DAP-seq targets in *P. stutzeri* WT, Δ*copR1*, Δ*copR2*, Δ*copR1copR2*, Δ*copSR2* and Δ*copR1copSR2* +/− copper chloride (Cu). qRT-PCR Cq-SEM < 1.0 for all samples reported.
B. Heatmap of the log$_2$ transcripts per million (TPM) as determined by RNA-seq analysis of zinc chloride (Zn) induced *P. stutzeri*, WT and Δ*czcR*. All genes are functionally annotated by blue for transport, yellow for sequestration, magenta for oxidases, gray for hypothetical or unknown function, red for RRs and green for HKs. All genes with 'stars' showed differential expression in the *copR* or *czcR* deletion experiments.

RR binding and suggest that these motifs are required for binding the RRs tested.

The large overlap of the CopR1 and CopR2 targeted genes, additional overlap in gene targets with CzcR, as well as the shared motif suggested an overlapping regulatory network for these regulators. To evaluate whether these observations were physiologically relevant, we tested if target genes responded when RCH2 was subjected to copper and zinc stress and if the response occurred in an RR-dependent manner (Fig. 3). We generated all the necessary gene deletion strains in the *copR1*, *copR2*, *copSR2* and *czcR* loci as well as a double *copR* mutant, Δ*copR1copR2* and Δ*copR1copSR2*. The RCH2 WT, Δ*copR1*, Δ*copR2*, Δ*copSR2* mutants as well as the Δ*copR1copR2* and Δ*copR1copSR2* strains were exposed to 50 μM copper chloride at mid-log phase for 1 h. The RNA of the corresponding cell pellets were used in a qRT-PCR assay using primers against the top DAP-seq gene targets of the CopR systems. In general, a minimum fold change of 2 (log$_2$ > 1) is needed in qRT-PCRs to be considered as changing. Only changes exceeding this cut-off were considered for discussion. Figure 3A shows the differential expression of these selected target genes in the presence or absence of copper stress in the WT as well as the RR mutants.

The qRT-PCR data (Fig. 3A) provides clear evidence for the physiological response of the DAP-seq gene
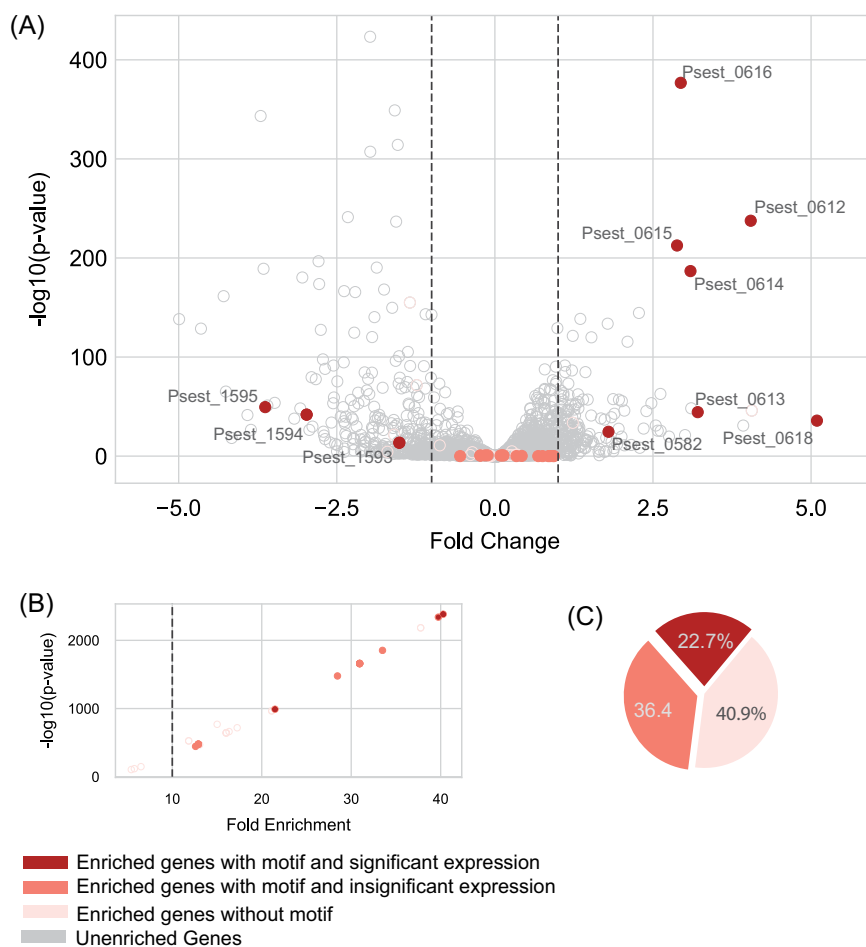
Fig. 4. RNA-seq data for WT and $\Delta czcR$ +/− zinc. Genes with RNA-seq fold-change $> +/- 1.5$, RNA-seq p-value < 0.001, Fold enrichment > 10 and DAP-seq p-value > 0.001 are represented in maroon. Genes below these thresholds with the conserved motif are represented in salmon, and genes below these thresholds without the motif are shown in light pink. Open gray circles represent all other genes. A. Volcano plot of differential expression WT + Zn^{2+} versus $\Delta czcR$ + Zn^{2+} annotated by DAP-seq data. Fold change cutoff is represented by hashed line. B. DAP-seq fold enrichment shown as a function of $\log_{10}.(p\text{-value})$ for each overlapping peak. Fold enrichment cutoff is represented by hashed line. C. Pie chart showing the percentage of genes within the DAP-seq data set above the statistical cut-off that contain the conserved motif and are also differentially expressed.

targets during copper stress in WT RCH2. The two *copR* genes were themselves mildly induced whereas Psest_0582, genes in the two *cop* operons (Psest_0583 and Psest_1589), the copper chaperone (Psest_1595), as well as Psest_1597 were very strongly induced. The two P-type ATPase transporter genes, Psest_0600 and Psest_1596, showed mild induction on copper stress. The zinc responsive genes *oprD* (Psest_0612) and *czcI* (Psest_0613) as well as Psest_0618 showed increases in expression, to different extents, during copper stress. In the absence of copper stress, neither the single nor the double *copR* deletions impacted the transcription of most selected DAP-seq target loci compared to the WT. An exception is Psest_1597 that showed a slight induction in the $\Delta copR1copR2$ strain even in the absence of copper stress. Under copper stress, Psest_0582, the most strongly induced gene during copper stress in WT, showed less induction in $\Delta copR1$, however it was strongly derepressed in the absence of CopR2 (in $\Delta copR2$ and $\Delta copR1copR2$). Deletion of *copR1* or *copR2* reduced induction of Psest_0583 (*copA1*) and of Psest_0587, suggesting that either CopR1 or CopR2 is

sufficient for the regulation of these genes. Interestingly, the opposite was true for Psest_1595, where deletions of either *copR1* or *copR2* derepressed this copper chaperone. The single deletion of *copR1* was sufficient to reduce induction of Psest_1589, whereas the single *copR2* deletion could reduce induction of Psest_1597. Most notably, the proposed zinc regulated genes *oprD* (Psest_0612), the *czcIABC* efflux pump (Psest_0613-6) and Psest_0618 were all highly derepressed in the absence of either CopR1 or CopR2.

The deletion of the histidine kinase (HK) *copS* and the RR *copR2* lowers the induction level of these genes to the WT plus copper levels. In the case of CopR1, if CopS was its sole HK, the $\Delta copSR2$ mutant, which lacks both the *copR2* and *copS* genes, should be expected to have the same phenotype as the $\Delta copR1copSR2$ double mutant. However, individual deletions in each of the two *copR* loci could not eliminate the full WT response to copper for several of the tested genes. In fact, the three-gene mutation $\Delta copR1copSR2$ is required to more broadly eliminate the WT response, such as the induction of Psest_0582,

0589 and 1597. Taken together this suggests that other kinases may be able to activate the CopR regulators. Our data is also consistent with study that examined the RB-TnSeq library of RCH2 under copper stress (Vaccaro *et al.*, 2016), where the individual disruptions in very few of the copper stress genes caused any fitness change, and this was attributed to the presence of functionally redundant paralogs.

The qRT-PCR measurement confirmed that both CopR1 and CopR2 regulate the RND-type zinc efflux transporter *czcIABC* genes (Psest_0613–0616) (Fig. 3A). To determine if CzcR also exhibited a crossregulatory architecture, we conducted a CzcR dependent expression analysis. Because of the large number of enriched targets for CzcR, we conducted RNA-seq to examine the response of these genes *in vivo*. Of the DAP-seq enriched genes (within the statistical cut-off and with a fold-enrichment > 10) 22.7% exhibited differential expression (Fig. 4B and C). 36.4% of genes enriched by CzcR have the motif, but were not differentially expressed. This result does not rule out the possibility that CzcR regulates these genes under different conditions or that the change in expression was too low to be successfully captured by RNA-seq. Importantly, the RNA-seq evaluation suggests that the presence of the motif, found by DAP-seq, is essential in determining which genes CzcR regulates under zinc stress (Fig. 4). Under Zn^{2+} exposure, and with the loss of an important regulatory protein, a large subset of genes is differentially expressed, shown in gray (Fig. 4A). The genes regulated by CzcR under Zn^{2+} exposure, shown in maroon, are clearly marked by the presence of the motif (Fig. 4A). Therefore, although the Zn^{2+} responsive genes in RCH2 extend much beyond the genes regulated by CzcR, all the operons regulated by this TCS (as identified using DAP-seq) contain the shared motif. The RNA-seq data reveals that CzcR induces expression of *czcIABC* genes (Psest_0613–0616). CzcR also induces expression of Psest_0618, but not the expression of the divergent gene Psest_0619 suggesting that only Psest_0618 is a true target (Fig. 3B). Zinc stress was also examined for RCH2 with the Rb-TnSeq RCH2 library (Vaccaro *et al.*, 2016). Consistent with our results, the *czcIABC* genes had fitness defect with Zn^{2+} stress, and so did Psest_0618 but not Psest_0619. An important finding is that in RCH2, along with *czcIABC*, CzcR also strongly induces *oprD* (Psest_0612) in response to zinc stress, contrasting what is known in *P. aeruginosa*, where CzcR represses *oprD* during Zn^{2+} stress (Caille *et al.*, 2007). The key copper homeostasis target operon that emerges as CzcR-regulated is Psest_1593–1595 encoding a putative ATPase transporter and copper chaperone. The expression of this operon is strongly derepressed in the *czcR* mutant during zinc stress suggesting that in the WT,
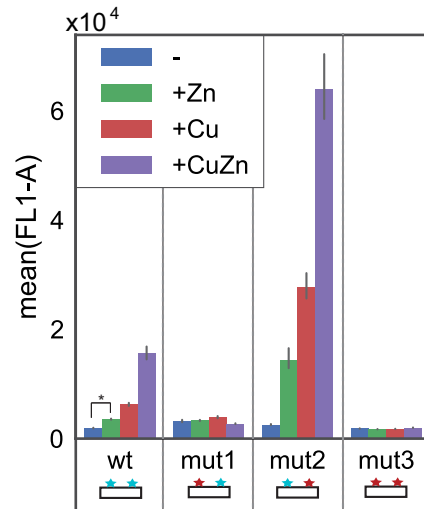

Fig. 5. CopR and CzcR distinguish between nearly identical motifs *in vivo*. A schematic of the Psest_0582 upstream sequence (white rectangle) of each reporter strain is shown below each strain name (wt, mut1, mut2 and mut3). A blue star indicates the native motif is present and a red star indicates that the native motif has been altered. Mean fluorescence (FL1-A) of 20,000 events per strain quantified after 24-h exposure to zinc chloride (Zn), copper chloride (Cu) or both (CuZn). $* = p$-val < 0.0001.

CzcR functions as a repressor at this locus. The data also shows that CzcR induces Psest_0582, another finding supportive of a crossregulatory architecture.

The mechanism of the observed crossregulation could be due to the similarity in the three RRs. Specifically, the percent identity of the DNA binding domains (DBD) of these three regulators is greater than 60% (Supporting Information Fig. S2), which raises the possibility that they bind similar DNA motifs. We examined the upstream regions of the genes regulated by the two CopRs and CzcR, and found that they each have two instances of the same DNA sequence motif. To confirm the dependence of gene regulation on these conserved motifs under zinc or copper stress *in vivo*, we developed a reporter assay using a plasmid based system that utilizes the upstream region of Psest_0582 to drive expression of green fluorescent protein (GFP). We observed that the presence of either zinc or copper induces the expression of GFP, as determined by single cell fluorescence activation and plate reader assays (Fig. 5 and Supporting Information Fig. S3). Next, we built three mutant variants of the Psest_0582 upstream region, where nucleotide substitutions were made in distal, proximal or both occurrences of the motif (Fig. 5 and Supporting Information Fig. S3A). We exposed each strain to either 50 μM copper chloride, 100 μM zinc chloride or both 50 μM copper chloride and 100 μM zinc chloride and monitored for GFP expression. Mutations in
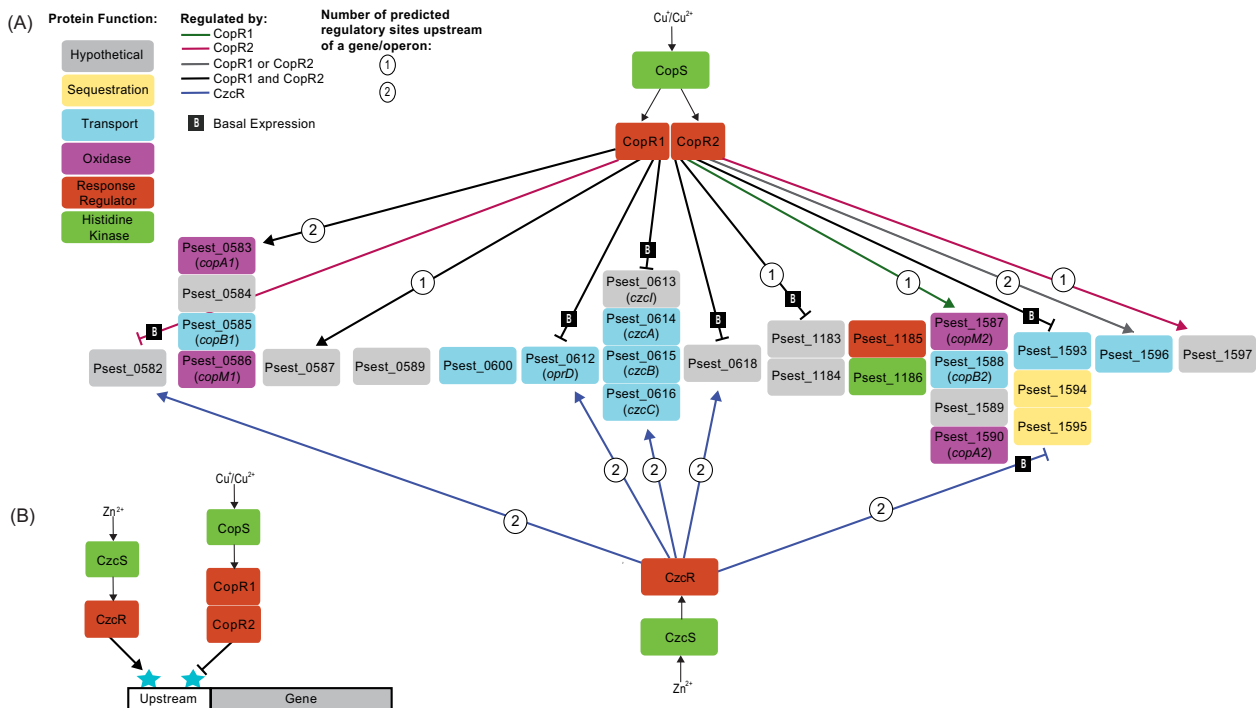
Fig. 6. Model for overlapping regulation by CopR1, CopR2 and CzcR.
A. Map of regulatory interactions for CopR1, CopR2 and CzcR. The regulatory network found by qRT-PCR and RNA-seq of copper chloride and zinc chloride induced mutant strains is depicted. CzcR regulates five operons, which have two copies of the motif.
B. Model for the observed motif bias in the upstream of genes regulated by CopR under copper stress and CzcR under zinc stress.

the distal site alone (mut1) or both the distal and proximal regulatory sites (mut3) led to complete loss of induction of Psest_0582 promoter by either copper, zinc or both metal ions (Fig. 5). However, mutations in the proximal site alone (mut2) resulted in increased expression in the presence of either copper or zinc and even greater induction by a combination of the two metals. Together these data suggest that under copper stress, CopR targets the distal motif for repression and an activating protein (possibly CzcR) targets the proximal motif. Interestingly, a similar mechanism for repression arises for regulation of this gene in the presence of zinc. Because a second regulator (possibly CopR) may be involved in repressing Psest_0582 while CzcR activates it during zinc exposure, there is additional support for regulatory crossregulation, where either the CzcS can phosphorylate both CzcR and CopR, CzcS and CopS are both activated by Zn^{2+}, or another regulator is activated to regulate this gene.

The *in vivo* validation of the DAP-seq results indicated a true overlapping regulatory structure for CopR1, CopR2 and CzcR. The presence of similar motifs in the upstream regions of DAP-seq gene targets for the three RRs potentially provides the key mechanism for the crossregulation of this set of genes. There are two main observations for the binding motifs observed. First, even

though the canonical motif for CopR1 and CopR2 are almost the same (Fig. 2B), we observed a different impact for regulation of genes by the two RRs (Figs 3, 5 and 6). Second, even though many CzcR DAP-seq targets share binding sites with the CopR regulators, per the RNA-seq data with the Δ*czcR* strain in zinc stress, CzcR only regulated a fraction of the genes that the CopR RRs regulate (Figs 3, 5 and 6). Notably, both CopR and CzcR repress genes Psest_1595 and Psest_1594, encoding an ATPase transporter and copper chaperone. This difference in subsets of genes regulated by each of the RRs can be manifested via a variety of mechanisms, ranging from difference in metal binding affinities and phosphorylating efficiency of the respective sensors, differences in the half-life of the phosphorylated RRs to differences in levels of protein expression, among other factors. Our dataset allowed us to assess if the specific binding motifs themselves or any chromosomal arrangements associated with the motifs may be responsible for these subsets. While no obvious and consistent difference in the distal versus the proximal motif is evident, we observed that the CzcR regulated genes typically contained two upstream binding sites, while the genes regulated by CopR1 and CopR2 may have either one or two sites (Fig. 6 and Supporting Information Table S1). Additional qRT-PCR

evaluation showed that the genes tested were induced more highly by zinc and copper together than by either of the two metals individually, suggesting that induction of these genes is stronger than the repression (Supporting Information Fig. S4).

The TCSs examined in this study likely only regulate a subset of genes involved in copper and zinc response. Both the earlier fitness study (Vaccaro *et al.*, 2016) and our CzcR RNA-seq suggest a much larger set of genes to be involved in RCH2 for copper and zinc homeostasis. Notably, *cue*, *cad* and *zur* genes have been identified in the RCH2 genome that may provide additional metal tolerance mechanisms (Chakraborty *et al.*, 2017). Functional categories known to dominate copper response are metal transport, oxidation and sequestration (Ladomersky and Petris, 2015). The specific genes targeted by CopR1, CopR2 and CzcR have a noteworthy representation of efflux systems and other transporters. Some of the targets (Psest_0600 and Psest_1596) belong to P-type ATPase family of transporters, which contains copper tolerance genes from *Escherichia coli* and other bacteria (Cha and Cooksey, 1991; Rowland and Niederweis, 2013). Interestingly, co-evolution of TCSs and transporters has been explored in Firmicutes TCS and ABC transport systems (Dintner *et al.*, 2011; Gebhard, 2012), and has also been observed in other bacteria (Singh *et al.*, 2014). The second prominent category of copper resistance genes involved in copper tolerance includes multicopper oxidases. The two CopA homologs regulated by the CopR1 and CopR2 belong to the multiple cupredoxin domain-containing SUF1 superfamily of proteins, and sufficiently fulfill this role. Other putative multicopper oxidoreductases [Psest_0710, Psest_0793 (Vaccaro *et al.*, 2016)] encoded in RCH2 are not targets for either of these three RRs. Two annotated putative copper chaperones represent the sequestration category of response. Lastly, two proteins, Psest_0582 and Psest_0618 annotated as 'hypothetical' are both highly regulated by CzcR and CopR. Analysis of the amino acid sequences show that both proteins have signal peptide sequences with cleavage sites between the 22nd and 23rd, 23rd and 24th amino acids respectively [Signal P, (Petersen *et al.*, 2011)]. The short amino acid sequences and metal dependent fitness (Vaccaro *et al.*, 2016) of these two proteins suggest that these proteins may be metal chaperones that aid in sequestering toxicity during metal exposure. The expression of these two potential chaperones shows a preference for Psest_0582 under copper stress, and for Psest_0618 under zinc stress (Supporting Information Fig. S4).

The RCH2 genome encodes numerous TCSs with 40 predicted HKs and 57 predicted RRs (pfam00072) [calculated using the MIST database, (Ulrich and Zhulin, 2007)]. Of these, 15 are RRs with a trans-reg-C (pfam00486) DNA-binding domain (DBD). A phylogenetic tree view of the DBDs of the 15 RRs reveal that four RRs form a closely related group (Supporting Information Fig. S2). This group includes the three RRs we have examined in this study as well as a fourth RR, Psest_1185. Psest_1185 is a DAP-seq target for CzcR. The qRT-PCR also confirmed Psest_1185-6 is a true target for both CopR1 and CopR2 during exposure to copper chloride (Supporting Information Fig. S5). Our study found that the binding motif upstream of Psest_1185 is synonymous to the CopR and CzcR motif, suggesting that these four regulators may all recruit the same set of genes using the common regulatory binding motif to form the core response to copper and zinc in RCH2.

Conclusions

Overlapping regulatory control is part of evolutionary refining for signal transduction cascades. In TCS, the dominant system of signaling in bacteria, such overlap occurs when multiple regulators are activated by one sensor kinase, or when a single regulator requires activation by more than one kinase (Jiang *et al.*, 2000; Laub and Goulian, 2007; Kaczmarczyk *et al.*, 2014; Rowland and Deeds, 2014). A response can also be modulated toward multiple related signals via other complex interactions between TCSs (Mitrophanov and Groisman, 2008). However, genes can also be regulated in response to more than one signal when regulatory motifs in the DNA binding sequence recruit regulators from multiple TCS. In this scenario, multiple RRs can regulate a core set of genes due to their common ability to bind upstream of their targets. Although less studied, this may be an equally important phenomenon in optimizing the response to signals that have synergistic or antagonistic consequence to the cell.

Environmental denitrifying bacteria are important for nitrate reduction and remediation, and they play a key role in anaerobic communities. These bacteria are also tolerant to a range of transition metals and serve as a model system for the examination of copper homeostasis and resistance (Lalucat *et al.*, 2006). Aggregating response to signals like transition metals is likely a scenario where multiple signaling cascades could be involved, and the importance of synergized response to copper and zinc ions has recently been observed in the pathogens *P. aeruginosa* (Caille *et al.*, 2007), *Enterococcus faecalis* (Latorre *et al.*, 2015) and *Acinetobacter baumannii* (Hassan *et al.*, 2017). Similar to our observations, the study in *A. baumannii* also reports the repression of copper uptake during zinc stress. Figure 6 outlines our major findings for TCS mediated response to copper and zinc in RCH2. A comprehensive study of three TCS

regulators allowed us to obtain a genome-wide view of their targets and discover their crossregulatory structure. The DAP-seq results were validated and further evaluated using qRT-PCR, RNA-seq and reporter assays, and gave us a view of the true targets of the RRs and their role as inducers or repressors. The data also highlights a potential epistatic hierarchy between CzcS and CopS. While CzcR and CopR may both be active during zinc and/or copper exposure, it remains to be examined if CzcR and CopR crosstalk with CzcS or CopS, or if CzcS and CopS have promiscuous ligand binding activity. The shared motifs between the three RRs not only confirms the mechanism of the crossregulation but also implicate a fourth closely related TCS in this shared response to the two transition metals. These aspects of the data further emphasize the need for genome-wide and comprehensive overviews of all TCS systems to understand regulatory networks, and discover the overlapping regulation in vital cellular responses.

Experimental procedures

Construction of expression strains

All RRs were cloned into pSKB3 plasmids with N-terminal 6X-His tags under T7 inducible promoters. The RRs were PCR amplified from the RCH2 gDNA with overhangs to the pSKB3 plasmid. Parts were assembled via Gibson assembly (Gibson *et al.*, 2009) and transformed into *E. coli* DH10b for plasmid propagation. The presence of the insert was confirmed by Sanger sequencing. Plasmids were purified and transformed into expression host *E. coli* BL21 (DE3). All primers used and plasmids generated are listed in Supporting Information Table S2.

Genomic DNA shearing

WT RCH2 was grown aerobically overnight in UGA media (Vaccaro *et al.*, 2016). UGA media contained 4.7 mM ammonium chloride, 1.3 mM potassium chloride, 2 mM magnesium sulfate, 0.1 mM calcium chloride, 0.3 mM sodium chloride, 5 mM sodium dihydrogen phosphate, 20 mM sodium lactate, 25 mM MOPS. Vitamins and minerals were added as described by Widdel and Bak (Widdel and Bak, 1992). Genomic DNA was prepared using the Wizard genomic kit (Promega, Wisconsin, MA) per manufacturer's instructions. Genomic DNA was sheared at 4°C in a Qsonica Q700 sonicator bath (Cole-Parmer, Vernon Hills, IL) Amp 90, 30s on 30s off pulse for 15 min to an average size distribution of 200–500 bp. The size distribution of the sheared genomic DNA was confirmed by gel electrophoresis.

Protein expression and purification

E. coli BL21 expression strains were grown overnight in Terrific broth (TB) + Kan media. 25 μl of overnight cultures were transferred to 10 ml TB media with Kan selection and grown at 37°C. Cultures were induced with 100–250 μM IPTG at OD_{600} 0.6–0.8 at 37°C and then incubated at 18°C for overnight expression. Samples were then pelleted and purified with TALON cobalt spin columns (Clontech, Mountainview, CA) per manufacturer's instructions. Purified proteins were desalted with desalting columns (GE Life sciences, Pittsburgh, PA) per manufacturer's instructions.

DAP protocol

Purified and desalted proteins were incubated with 500 ng sheared DNA, 1 μM DTT, 10 mM MgCl2, with a reaction volume of 100 μl in PBS (50 mM NaCl, 27 mM KCl, 100 mM Na_2HPO_4, 18 mM KH_2PO_4, pH 7.2) for a half hour or 1 h if 50 μM Acetyl-PO_4 was added for *in vitro* phosphorylation of the RRs. DNA bound to His-tagged protein was then enriched with 30 μl HisPur Ni-NTA resin (Thermo Scientific, Waltham, MA) incubated by shaking for 30 min. The resin was washed 3 times with 200 μl PBS buffer and eluted with 100 μl of PBS buffer with 500 μM imidazole. Input samples were not affinity purified. DNA was purified with 1.2X AMPure beads (Agilent, Santa Clara, CA), and eluted into 35 μl 0.1X TE (1 mM Tris-HCl, 0.1 mM EDTA, pH 8). Complete list of DAP samples is provided in the Supporting Information data file.

DAP-seq library prep

DAP enriched and input samples were processed using the NEB Next Ultra II library prep kit (New England Biolabs, Ipswich, MA) per the manufacturer's instructions with a 200 bp size selection. Size distribution of individual DAP-seq samples were assessed with the DNA high sensitivity kit on the Bioanalyzer (Agilent Technologies, Santa Clara, CA). Individual sample concentrations were quantified with NEB library quantification kit (New England Biolabs, Ipswich, MA), per the manufacturer's instructions. Samples were then combined to a final concentration of 10 nM and sequenced for 150 cycles on a MiSeq with the Miseq reagent kit v3 (Illumina, San Diego, CA).

DAP-seq analysis

Low quality bases were trimmed and reads shorter than 30 bp were filtered out using SolexaQA++ v3.1.6 (Cox *et al.*, 2010). DAP-seq and input reads were mapped to the RCH2 reference genome using Bowtie v1.1.2 (Langmead *et al.*, 2009) with –m 1 parameter (report reads with single alignment only). Resulting SAM files were converted to BAM format and sorted using samtools v 0.1.19 (Li *et al.*, 2009). Peak calling was performed using MACS2 (Zhang *et al.*, 2008) with –nomodel, – extsize 250, – keep-dup = all parameters and *q*-value threshold of 0.0001. Peak sequences were extracted, nearest genes for peaks were annotated and peak positions between samples were compared using in-house Perl scripts. Enriched motifs were discovered in peak sequences using MEME (Bailey *et al.*, 2009).

DPI-ELISA

Biotinylated top strand oligonucleotides and unlabeled complementary bottom strand oligonucleotides were annealed together by mixing them in 1:1.5 ratio in 10 mM Tris-HCl, pH 8, 50 mM NaCl, 1 mM EDTA and heating to 95°C for 5 min followed by slow cooling to 25°C with a hold at 55°C for 5 min. The DPI-ELISA protocol was adapted from Brand *et al.* (2010). 2.5 pmol of the biotin-labeled DNA substrate was dissolved in a total of 60 μl TBS-T (20 mM Tris-HCl pH 7.5, 100 mM NaCl, 0.1%(v/v) Tween-20) and added to each well of a Pierce streptavidin-coated clear 96-well plate (Thermo Fisher Scientific, Waltham, MA). The plate was incubated at 37°C for 1 h. The wells were washed three times with 150 μl of TBS-T. Blocking buffer (3% BSA in TBS; 100 μl) was added to each well and incubated on the bench for 30 min. The wells were washed with 3 × 150 μl TBS-T. Protein mix (60 μl per well) was prepared in triplicate by diluting 10 μl of protein in 10 mM Tris HCl pH 7.5, 5 mM MgCl$_2$, 50 mM KCl, 1 mM DTT, 2 μg poly dI.dC. The protein mix was added to each well and then incubated at RT for 30 min, followed by washing 3X with 150 μl of TBS-T buffer. Ni-NTA HRP conjugate (Qiagen, Hilden, Germany) was diluted 1:1000 in TBS-T buffer, and 60 μl of the diluted stock was added per well. The plate was incubated for 1 h at RT and washed 2X 150 μl TBS-T and 2X 150 μl TBS. An OPD (o-Phenylenediamine dihydrochloride) tablet (20 mg) (Sigma, St. Louis, MO) was dissolved in 30 ml CP buffer (10 mM Na$_2$HPO4, 100 mM citric acid, pH 5 with NaOH) with 150 μl of 3% H$_2$O$_2$. 60 μl OPD solution was added per well, and incubated in the dark on the bench for 5–10 min. The reaction was stopped with 60 μl of stopping solution (2N HCl), the plate was kept in dark on an orbital shaker for 5 min. The absorbance was measured at 492 nm on a Spectramax plate reader (Molecular Devices, Sunnyvale, CA). OPD solution plus stopping solution was used as a blank.

Construction of RCH2 deletion mutants

RCH2 mutants were constructed by marker exchange. Unstable marker exchange plasmids were constructed for each deletion by assembling 4 PCR products by Gibson assembly. PCR products were amplified by the DiVA PCR service (diva.jbei.org, Supporting Information Table S2). Each Gibson assembly consisted of (1) plasmid backbone PCR product (pUC origin of replication and spectinomycin resistance gene), (2) kanamycin resistance gene flanked by (3) 500 bp upstream and (4) 500 bp downstream of the gene to be deleted. The Gibson reactions were transformed into *E. coli* DH10b cells and selected on LB-Spec-Kan. The constructs were verified to contain all four parts by sequencing and colony PCR. Electrocompetent RCH2 cells were prepared as follows: Cells (50 ml) were grown overnight aerobically in LC medium (10 g l^{-1} tryptone, 5 g l^{-1} NaCl, 5 g l^{-1} yeast extract). The cells were chilled on ice and centrifuged. The cell pellets were washed twice in cold 300 mM sucrose (33 ml), followed by resuspension in 3.3 ml of 300 mM sucrose. The cells were frozen in 100 μl aliquots and stored at −80°C. The marker exchange plasmids were transformed into electrocompetent RCH2 as

follows: 100 ng of plasmid was mixed with 100 μl cells and the mixture was electroporated in 1 mm gapped cuvettes (1250 V, 200 Ω, 25 μF). The cells were recovered in 300 μl LB overnight at 30°C and transformants were selected on LB-Kan. Kan resistant colonies were screened for spectinomycin sensitivity by patching colonies on LB-Spec plates. Genomic DNA was isolated from three Kan-resistant Spec-sensitive transformants for each deletion. The deletion was verified by qRT-PCR with gDNA as template and select primers for the deleted gene, the kanamycin-resistance gene and primers for control genes (*rpoD*). To create the double knockout of *copR1* and *copR2* genes, a marker exchange plasmid was constructed with the pUC origin of replication and the 500 bp fragments upstream and downstream of *copR1* flanking the spectinomycin resistance gene. The PCR fragments were assembled by Gibson assembly into *E. coli* DH10b and transformants were selected on LB-Spec. Sequence verified plasmid was transformed into electrocompetent *copR2* and *copSR2* RCH2 deletion strain, and transformants were selected on LB-Kan-Spec. A few colonies were screened by colony qRT-PCR with primers targeting *copR1*, *copR2*, *copS* and *rpoD* genes to verify deletions. Primers used and plasmids generated are listed in Supporting Information Table S2.

Copper and zinc stress

For zinc stress experiments, WT RCH2 and *czcR* mutant strains were each grown aerobically from overnight cultures in six tubes of 6 ml UGA (Vaccaro *et al.*, 2016) medium (+ Kan for the mutant) at 30°C with shaking. To determine the optimal stress concentration used in subsequent experiments, 500 μl WT RCH2 was exposed to copper and zinc in varying concentrations ranging from 400 μM to 6.25 μM. OD$_{600}$ was monitored kinetically, in triplicate, with the TecanF200 (Tecan Trading AG, Mannedorf, Switzerland) (Supporting Information Fig. S6). At an OD$_{600}$ of 0.2, three of the WT tubes and three of the *czcR* mutant tubes received 100 μM of zinc chloride. The remaining three tubes of each strain received nothing. After incubation at 30°C for an hour, 1.5 ml aliquots of each culture were removed and mixed with 2X the volume of Bacteria protect reagent (Qiagen, Hilden, Germany).

For copper stress experiments, WT RCH2, *copR1*, *copSR2* and *copR1-copSR2* mutant strains were each grown aerobically from overnight cultures in six tubes of 6 ml UGA (Vaccaro *et al.*, 2016) medium (+ appropriate antibiotics for the mutant) at 30°C with shaking. At an OD$_{600}$ of 0.2, three tubes for each strain received 50 μM of copper(II) chloride, and were incubated for an hour at 30°C. 1.5 ml culture aliquots were removed from each tube and mixed with 2X the volume of Bacteria protect reagent (Qiagen, Hilden, Germany).

RNA isolation and qRT-PCR

The mixture of cells and RNA protect reagent (Qiagen, Hilden, Germany) was centrifuged at 9000 *g* for 15 min. Cells were lysed with lysozyme and RNA was isolated with the RNeasy mini spin kit (Qiagen, Hilden, Germany) following

manufacturer's instructions. The RNA was treated with Turbo DNA-free kit (Thermo Fisher, Waltham, MA) to remove any genomic DNA contamination. RNA concentrations were measured on the Nanodrop (Thermo Fisher, Waltham. MA) and RNA integrity was verified with the RNA 6000 Nano kit on the Bioanalyzer (Agilent Technologies, Santa Clara. CA). RNA (250 ng) was reverse transcribed with the iScript RT Supermix (Bio-Rad, Hercules, CA), and the resulting cDNA was diluted fourfold for use as template in qRT-PCR reactions. Each qRT-PCR reaction (5 μl) contained 1 μl of template DNA, 0.25 μl of each primer (10 μM) and 2.5 μl of 2X SsoAdvanced Universal SYBR Green mix (Bio-Rad, Hercules, CA). qRT-PCR reactions were assembled on a Bio-Rad 384-well hard shell plate with the Echo liquid handler (Lab-Cyte, San Jose, CA), and the reactions were run on a CFX384 instrument (Bio-Rad, Hercules, CA). Primers used are listed in Supporting Information Table S3.

RNA-seq library prep

DNA-free RNA was isolated as described above for qRT-PCR. RNA concentrations were measured on the Nanodrop (Thermo Fisher, Waltham. MA) and RNA integrity was verified with the RNA 6000 Nano kit on the Bioanalyzer (Agilent Technologies, Santa Clara. CA). Structural rRNAs were then removed using the Bacterial RiboMinus Transcriptome Isolation kit (Thermo Fisher, Waltham. MA), and concentrated with RNeasy mini spin kit (Qiagen, Hilden, Germany). Libraries for RNAseq were prepared using the NEBnext kit Ultra RNA library prep kit for Illumina (New England Biolabs, Ipswich, MA) per manufacturer's instructions. Individual sample quality was determined by DNA high sensitivity kit on the Bioanalyzer (Agilent Technologies, Santa Clara, CA). Sample concentrations were quantified with NEB library quantification kit (New England Biolabs, Ipswich, MA). Samples were then combined to a final concentration of 10 nM and sequenced on a MiSeq reagent kit v3, using 150 cycles of paired end reads.

RNA-seq analysis

FASTQ files generated from Illumina reads were mapped onto RCH2 coding sequences using Kallisto version 0.42.5 (Bray *et al.*, 2016). Transcripts per million (TPM) and differential gene expression analyses were conducted using the R package sleuth version 0.28.1 (Pimentel *et al.*, 2017). Bacterial operons were predicted from RNA-seq data using Rockhopper 2 (Tjaden, 2015).

Construction of reporter plasmids

The Psest_0582 promoter was amplified from the 400 bp sequence upstream of Psest_0582 start codon from RCH2 genomic DNA with overhangs to a pBAD plasmid housing WT-GFP and a spectinomycin resistance marker. This plasmid was constructed by Gibson assembly (Gibson *et al.*, 2009) and was transformed into chemically competent *E. coli* DH10b for propagation. The mutant p0582 promoters were synthesized by IDT (Integrated DNA Technologies,

Redwood City, CA) and were constructed in the same manner as the WT promoter. After sequence confirmation, the plasmids were transformed into RCH2 WT by electroporation followed by selection on spectinomycin. Colonies were screened for the presence of the plasmid by colony PCR. Triplicates of each reporter strain were selected for screening.

Fluorescent reporter screen

WT 0582 and mutant 0582 reporter strains were grown overnight in UGA +spec medium. The strains were back diluted in 10 ml to an OD_{600} of 0.1 and grown to OD_{600} 0.2 at 30°C. 500 μl of each strain in replicate was then transferred to a 48-well plate. Each replicate received, in duplicate, zinc chloride, copper chloride, or both to a final concentration of 100 μM or 50 μM respectively. Control wells received nothing. The plates were monitored on the Biotek synergy H4 (Biotek, Winooski, VT) with absorbance settings set to read OD_{600} and fluorescence parameters set to excitation and absorbance of 485/20 and 518/20 respectively. After 24-h of growth in the Biotek, cultures were transferred to a 96 deep-well plate and monitored on the BD accuri (BD biosciences, San Jose, CA) for single cell fluorescence endpoint analysis.

Phylogenetic analysis

To characterize the relatedness of the DNA binding domains of response regulators in RCH2 we used hmmsearch from HMMER v3.1b2 to identify all proteins that contained a Trans_reg_C domain using the Trans_-reg_C hmm from xfam (Mistry *et al.*, 2013). Domain sequences were extracted from whole sequences based on coordinates determined by the hmmsearch via a custom python script. We aligned domains using the MAFFT-LINSI algorithm from MAFFT v7.310 (Katoh and Standley, 2013). Conserved amino acids within the domains were visualized using UniPro UGENE software v1.25.0 (Okonechnikov *et al.*, 2012). Phylogenetic trees were constructed using FastTree 2 (Price *et al.*, 2010), and trees were visualized using the web interface iTOL (Letunic and Bork, 2016).

Conflict of Interest

The authors declare no conflict of interest.

Acknowledgements

References

Bailey, T.L., Boden, M., Buske, F.A., Frith, M., Grant, C.E., Clementi, L., *et al*. (2009) MEME SUITE: tools for motif discovery and searching. *Nucleic Acids Res* **37**: W202–W208.

Brand, L.H., Kirchler, T., Hummel, S., Chaban, C., and Wanke, D. (2010) DPI-ELISA: a fast and versatile method to specify the binding of plant transcription factors to DNA in vitro. *Plant Methods* **6**: 25.

Bray, N.L., Pimentel, H., Melsted, P., and Pachter, L. (2016) Near-optimal probabilistic RNA-seq quantification. *Nat Biotechnol* **34**: 525–527.

Caille, O., Rossier, C., and Perron, K. (2007) A copper-activated two-component system interacts with zinc and imipenem resistance in *Pseudomonas aeruginosa*. *J Bacteriol* **189**: 4561–4568.

Cha, J.S., and Cooksey, D.A. (1991) Copper resistance in *Pseudomonas syringae* mediated by periplasmic and outer membrane proteins. *Proc Natl Acad Sci USA* **88**: 8915–8919.

Chakraborty, R., Woo, H., Dehal, P., Walker, R., Zemla, M., Auer, M., *et al*. (2017) Complete genome sequence of *Pseudomonas stutzeri* strain RCH2 isolated from a Hexavalent Chromium [Cr(VI)] contaminated site. *Stand Genomic Sci* **12**: 23.

Chandrangsu, P., Rensing, C., and Helmann, J.D. (2017) Metal homeostasis and resistance in bacteria. *Nat Rev Microbiol* **15**: 338–350.

Cox, M.P., Peterson, D.A., and Biggs, P.J. (2010) SolexaQA: at-a-glance quality assessment of Illumina second-generation sequencing data. *BMC Bioinformatics* **11**: 485.

Crooks, G.E., Hon, G., Chandonia, J.M., and Brenner, S.E. (2004) WebLogo: a sequence logo generator. *Genome Res* **14**: 1188–1190.

Dintner, S., Staron, A., Berchtold, E., Petri, T., Mascher, T., and Gebhard, S. (2011) Coevolution of ABC transporters and two-component regulatory systems as resistance modules against antimicrobial peptides in Firmicutes Bacteria. *J Bacteriol* **193**: 3851–3862.

Gebhard, S. (2012) ABC transporters of antimicrobial peptides in Firmicutes bacteria—phylogeny, function and regulation. *Mol Microbiol* **86**: 1295–1317.

Gibson, D.G., Young, L., Chuang, R.Y., Venter, J.C., Hutchison, C.A., III, and Smith, H.O. (2009) Enzymatic assembly of DNA molecules up to several hundred kilobases. *Nat Methods* **6**: 343–345.

Hassan, K.A., Pederick, V.G., Elbourne, L.D., Paulsen, I.T., Paton, J.C., McDevitt, C.A., and Eijkelkamp, B.A. (2017) Zinc stress induces copper depletion in *Acinetobacter baumannii*. *BMC Microbiol* **17**: 59.

Hoegger, P.J., Kilaru, S., James, T.Y., Thacker, J.R., and Kues, U. (2006) Phylogenetic comparison and classification of laccase and related multicopper oxidase protein sequences. *FEBS J* **273**: 2308–2326.

Jiang, M., Shao, W., Perego, M., and Hoch, J.A. (2000) Multiple histidine kinases regulate entry into stationary phase and sporulation in *Bacillus subtilis*. *Mol Microbiol* **38**: 535–542.

Kaczmarczyk, A., Hochstrasser, R., Vorholt, J.A., and Francez-Charlot, A. (2014) Complex two-component signaling regulates the general stress response in Alphaproteobacteria. *Proc Natl Acad Sci USA* **111**: E5196–E5204.

Katoh, K., and Standley, D.M. (2013) MAFFT multiple sequence alignment software version 7: improvements in performance and usability. *Mol Biol Evol* **30**: 772–780.

Ladomersky, E., and Petris, M.J. (2015) Copper tolerance and virulence in bacteria. *Metallomics* **7**: 957–964.

Lalucat, J., Bennasar, A., Bosch, R., Garcia-Valdes, E., and Palleroni, N.J. (2006) Biology of *Pseudomonas stutzeri*. *Microbiol Mol Biol Rev* **70**: 510–547.

Langmead, B., Trapnell, C., Pop, M., and Salzberg, S.L. (2009) Ultrafast and memory-efficient alignment of short DNA sequences to the human genome. *Genome Biol* **10**: R25.

Latorre, M., Low, M., Garate, E., Reyes-Jara, A., Murray, B.E., Cambiazo, V., and Gonzalez, M. (2015) Interplay between copper and zinc homeostasis through the transcriptional regulator Zur in *Enterococcus faecalis*. *Metallomics* **7**: 1137–1145.

Laub, M.T., and Goulian, M. (2007) Specificity in two-component signal transduction pathways. *Annu Rev Genet* **41**: 121–145.

Letunic, I., and Bork, P. (2016) Interactive tree of life (iTOL) v3: an online tool for the display and annotation of phylogenetic and other trees. *Nucleic Acids Res* **44**: W242–W245.

Li, H., Handsaker, B., Wysoker, A., Fennell, T., Ruan, J., Homer, N., *et al*. (2009) The sequence alignment/map format and SAMtools. *Bioinformatics* **25**: 2078–2079.

Lin, X., Kennedy, D., Peacock, A., McKinley, J., Resch, C.T., Fredrickson, J., and Konopka, A. (2012) Distribution of microbial biomass and potential for anaerobic respiration in Hanford Site 300 Area subsurface sediment. *Appl Environ Microbiol* **78**: 759–767.

Long, F., Su, C.C., Zimmermann, M.T., Boyken, S.E., Rajashankar, K.R., Jernigan, R.L., and Yu, E.W. (2010) Crystal structures of the CusA efflux pump suggest methionine-mediated metal transport. *Nature* **467**: 484–488.

Mistry, J., Finn, R.D., Eddy, S.R., Bateman, A., and Punta, M. (2013) Challenges in homology search: HMMER3 and convergent evolution of coiled-coil regions. *Nucleic Acids Res* **41**: e121.

Mitrophanov, A.Y., and Groisman, E.A. (2008) Signal integration in bacterial two-component regulatory systems. *Genes Dev* **22**: 2601–2611.

O'Malley, R.C., Huang, S.S., Song, L., Lewsey, M.G., Bartlett, A., Nery, J.R., *et al.* (2016) Cistrome and epicistrome features shape the regulatory DNA landscape. *Cell* **165**: 1280–1292.

Okonechnikov, K., Golosova, O., Fursov, M., and Team, U. (2012) Unipro UGENE: a unified bioinformatics toolkit. *Bioinformatics* **28**: 1166–1167.

Petersen, T.N., Brunak, S., von Heijne, G., and Nielsen, H. (2011) SignalP 4.0: discriminating signal peptides from transmembrane regions. *Nat Methods* **8**: 785–786.

Pezza, A., Pontel, L.B., Lopez, C., and Soncini, F.C. (2016) Compartment and signal-specific codependence in the transcriptional control of Salmonella periplasmic copper homeostasis. *Proc Natl Acad Sci USA* **113**: 11573–11578.

Pimentel, H., Bray, N., Puente, L., Melsted, S.P., and Pachter, L. (2017) Differential analysis of RNA-seq incorporating quantification uncertainty. *Nat Methods* **14**: 687–690.

Price, M.N., Dehal, P.S., Arkin, A.P., and Poon, A.F.Y. (2010) FastTree 2–approximately maximum-likelihood trees for large alignments. *PLoS One* **5**: e9490.

Rajeev, L., Luning, E.G., Dehal, P.S., Price, M.N., Arkin, A.P., and Mukhopadhyay, A. (2011) Systematic mapping of two component response regulators to gene targets in a model sulfate reducing bacterium. *Genome Biol* **12**: R99.

Rajeev, L., Luning, E.G., and Mukhopadhyay, A. (2014) DNA-affinity-purified chip (DAP-chip) method to determine gene targets for bacterial two component regulatory systems. *J Vis Exp* (**89**).

Rowland, J.L., and Niederweis, M. (2013) A multicopper oxidase is required for copper resistance in *Mycobacterium tuberculosis*. *J Bacteriol* **195**: 3724–3733.

Rowland, M.A., and Deeds, E.J. (2014) Crosstalk and the evolution of specificity in two-component signaling. *Proc Natl Acad Sci USA* **111**: 5550–5555.

Singh, K., Senadheera, D.B., and Cvitkovitch, D.G. (2014) An intimate link: two-component signal transduction systems and metal transport systems in bacteria. *Future Microbiol* **9**: 1283–1293.

Somenahally, A.C., Mosher, J.J., Yuan, T., Podar, M., Phelps, T.J., Brown, S.D., *et al.* (2013) Hexavalent chromium reduction under fermentative conditions with lactate stimulated native microbial communities. *PLoS One* **8**: e83909.

Su, C.C., Long, F., and Yu, E.W. (2011) The Cus efflux system removes toxic ions via a methionine shuttle. *Protein Sci* **20**: 6–18.

Thorgersen, M.P., Lancaster, W.A., Vaccaro, B.J., Poole, F.L., Rocha, A.M., Mehlhorn, T., *et al.* (2015) Molybdenum Availability Is Key to Nitrate Removal in Contaminated Groundwater Environments. *Appl Environ Microbiol* **81**: 4976–4983.

Tjaden, B. (2015) De novo assembly of bacterial transcriptomes from RNA-seq data. *Genome Biol* **16**: 1.

Ulrich, L.E., and Zhulin, I.B. (2007) MiST: a microbial signal transduction database. *Nucleic Acids Res* **35**: D386–D390.

Vaccaro, B.J., Lancaster, W.A., Thorgersen, M.P., Zane, G.M., Younkin, A.D., Kazakov, A.E., *et al.* (2016) Novel metal cation resistance systems from mutant fitness analysis of denitrifying *Pseudomonas stutzeri*. *Appl Environ Microbiol* **82**: 6046–6056.

Widdel, F., and Bak, F. (1992) Gram-negative mesophilic sulfate-reducing bacteria. In *The Prokaryotes: A Handbook on the Biology of Bacteria: Ecophysiology, Isolation, Identification, Applications*. Balows, A., Trüper, H.G., Dworkin, M., Harder, W., and Schleifer, K.-H. (eds). New York, NY: Springer New York, pp. 3352–3378.

Zhang, Y., Liu, T., Meyer, C.A., Eeckhoute, J., Johnson, D.S., Bernstein, B.E., *et al.* (2008) Model-based analysis of ChIP-Seq (MACS). *Genome Biol* **9**: R137.

Supporting information

Additional supporting information may be found in the online version of this article at the publisher's web-site.